

1 Passive Sampling to Capture the Spatial Variability of
2 Coarse Particles by Composition in Cleveland, OH

3
4 Eric J. Sawvel^a, Robert Willis^b, Roger R. West^c, Gary Casuccio^c, Gary Norris^b,
5 Naresh Kumar^d, Davyda Hammond^e, and Thomas M. Peters^{a,f}

6
7 ^a The University of Iowa, Iowa City, IA

8 ^b US EPA, Office of Research and Development, National Exposure Research Laboratory,
9 Research Triangle Park, NC, USA

10 ^c RJ Lee Group, Inc., Monroeville, PA

11 ^d University of Miami, Miami, FL

12 ^e Oak Ridge Associated Universities, Oak Ridge, TN

13 ^f Corresponding author: 145 N Riverside Drive, S331 CPHB, University of Iowa, Iowa City, IA,
14 thomas-m-peters@uiowa.edu

15 **KEYWORDS**

16 PM_{10-2.5}, particulate matter, computer controlled scanning electron microscopy, single particle
17 analysis

18 **ABSTRACT**

19 Passive samplers deployed at 25 sites for three, week-long intervals were used to characterize
20 spatial variability in the mass and composition of coarse particulate matter (PM_{10-2.5}) in
21 Cleveland, OH in summer 2008. The size and composition of individual particles determined
22 using computer-controlled scanning electron microscopy with energy-dispersive X-ray
23 spectroscopy (CCSEM-EDS) was then used to estimate PM_{10-2.5} concentrations ($\mu\text{g m}^{-3}$) and its
24 components in 13 particle classes. The highest PM_{10-2.5} mean mass concentrations were
25 observed at three central industrial sites ($35 \mu\text{g m}^{-3}$, $43 \mu\text{g m}^{-3}$, and $48 \mu\text{g m}^{-3}$), whereas
26 substantially lower mean concentrations were observed to the west and east of this area at
27 suburban background sites ($13 \mu\text{g m}^{-3}$ and $15 \mu\text{g m}^{-3}$). PM_{10-2.5} mass and components associated
28 with steel and cement production (Fe-oxide and Ca-rich) exhibited substantial heterogeneity
29 with elevated concentrations observed in the river valley, stretching from Lake Erie south
30 through the central industrial area and in the case of Fe-oxide to a suburban valley site. Other
31 components (e.g., Si/Al-rich typical of crustal material) were considerably less heterogeneous.
32 This work shows that some species of coarse particles are considerably more spatially

1 heterogeneous than others in an urban area with a strong industrial core. It also demonstrates
2 that passive sampling coupled with analysis by CCSEM-EDS is a useful tool to assess the spatial
3 variability of particulate pollutants by composition.

4 **1. INTRODUCTION**

5 Exposure to fine atmospheric particulate matter ($PM_{2.5}$) has been associated with increased
6 adverse cardiopulmonary health effects (Brook, Rajagopalan et al. 2010, Hoek, Krishnan et al.
7 2013), although effect estimates vary significantly among studies with heterogeneity in fine
8 particle composition suspected as a factor of considerable uncertainty (Hoek, Krishnan et al.
9 2013). The evidence is less clear for adverse health effects associated with exposure to coarse
10 particulate matter ($PM_{10-2.5}$), with recent meta-analyses reporting a lack of evidence for
11 mortality (Hoek, Krishnan et al. 2013), but ‘suggestive evidence’ for increased morbidity and
12 mortality not explained by simultaneous co-exposure to $PM_{2.5}$ (Adar, Filigrana et al. 2014). These
13 meta-analyses stress the need to better characterize the heterogeneity of particulate matter
14 exposures by composition to reduce uncertainty in effect estimates, especially for $PM_{10-2.5}$.

15 The combination of varying sources and short atmospheric lifetimes often leads to substantial
16 heterogeneity in the concentration and chemical makeup of $PM_{10-2.5}$. Coarse atmospheric
17 particles are emitted primarily by widely varying mechanical and resuspension sources, leading
18 to a complex mixture of material from roads, soil, wear of automotive parts (e.g., tires and
19 brakes), and biological material from vegetation (Kelly and Fussell 2012). Particle settling
20 velocity scales with diameter squared causing coarse particles to settle substantially faster than
21 fine particles (Seinfeld and Pandis 2012, Zhang and He 2014). Consequently, the use of data
22 from spatially sparse networks of regulatory samplers can result in substantial exposure
23 misclassification for $PM_{10-2.5}$ that can attenuate the power of epidemiological studies (Chang,
24 Peng et al. 2011).

25 Networks of active samplers—samplers that collect particles from an aspirated volume of air—
26 have been used to measure the spatial variability of $PM_{10-2.5}$ in urban settings. Burton, Suh et al.
27 (1996) used paired PM_{10} and $PM_{2.5}$ filter samplers at eight sites to show that coarse particles
28 (calculated by subtraction: $PM_{10} - PM_{2.5}$) were heterogeneously distributed across Philadelphia,
29 PA. This subtraction method, however, is subject to multiple measurement error from two filter
30 samplers, introducing measurement uncertainty in gravimetric measurement that is amplified in
31 chemical analysis (Goldman, Mulholland et al. 2011). Using a two impactors in series,
32 Thornburg, Rodes et al. (2009) measured coarse particles separately from particles of other size.
33 They found that $PM_{10-2.5}$ measured at five sites in Detroit, MI were temporally correlated and
34 had low spatial heterogeneity. The spatial heterogeneity of $PM_{10-2.5}$ and its components has
35 been studied intensively in Los Angeles, CA with networks of cascade impactors (Cheung, Daher
36 et al. 2011, Cheung, Olson et al. 2012, Fruin, Urman et al. 2014). At 10 downtown and suburban
37 sites, $PM_{10-2.5}$ mass was observed to be moderately heterogeneous (Pakbin, Hudda et al. 2010)
38 with greater heterogeneity observed for components of coarse particles (Cheung, Daher et al.

1 2011, Cheung, Olson et al. 2012). [ENREF 7](#) Fruin, Urman et al. (2014) identified substantial
2 within-community heterogeneity in PM_{10-2.5}.

3 Networks of passive samplers have been used to investigate the spatial and temporal variability
4 in PM_{10-2.5}. Compared to active sampling, passive samplers are relatively inexpensive, require no
5 electricity to operate, and can be deployed at numerous locations easily and cost-effectively
6 (Wagner and Leith 2001a). Ott, Kumar et al. (2008) used passive samplers at 30 sites with
7 analysis by light microscopy to show that coarse PM was highly heterogeneous at a spatial scale
8 of 4.4 km in a medium-sized Midwest city. Lagudu, Raja et al. (2011) used a network of 25
9 passive samplers with analysis by computer-controlled scanning electron microscopy
10 coupled with energy-dispersive X-ray spectrometry (CCSEM-EDS) to show PM_{10-2.5} mass and
11 its components were highly heterogeneous at a spatial scale of 2 km across Rochester,
12 NY.

13 Less work has been done to assess the spatial heterogeneity of PM_{10-2.5} in cities with substantial
14 industrial activity, such as Cleveland, OH. Cleveland, OH is a 'rust belt' city with substantial steel
15 and cement production in a central river valley. In a previous publication, the spatial
16 heterogeneity of iron-containing particles within the Cleveland metropolitan area was
17 investigated using arrays of passive samplers analyzed by CCSEM-EDS (Ault, Peters et al. 2012).
18 Results indicated that anthropogenic iron-containing coarse particles were highly
19 heterogeneous and subject to physicochemical transformation as they moved away from their
20 source.

21 The goal of the present work was to more broadly investigate the spatial heterogeneity of PM₁₀₋
22 _{2.5} mass and compositional components in Cleveland, OH using a network of passive samplers
23 coupled with single particle analysis by CCSEM-EDS. Particles were classified into 13
24 compositional classes based on their X-ray spectra. The spatial variability of PM_{10-2.5} and the 13
25 components were evaluated with visual and quantitative indicators of heterogeneity. We report
26 that anthropogenic particles from the industrial core are more heterogeneous than crustal
27 material. These results may be important for interpreting epidemiological data for cities with
28 strong industrial cores. Moreover, passive sampling with single particle analysis represents an
29 alternative exposure assessment method for the epidemiology of PM_{10-2.5}.

30 **2. METHODS**

31 **2.1 Study Area**

32 Sampling was conducted in the Cleveland, OH metropolitan area (Figure 1). Included in the
33 study area is Cleveland's Flats District, a low-lying topography along the banks of the lower
34 Cuyahoga River from the river's mouth at Lake Erie stretching south approximately 8 km. The
35 elevation of the river surface is approximately 180 m above sea level. The surrounding bluffs
36 start at an elevation of 213 m and extend to a height of approximately 365 m above sea level.

1 The river valley width varies from 0.8 km at its narrowest point and widens to approximately 2.4
2 km.

3 Within the Flats, large quantities of steel are produced by integrated and electric arc furnace.
4 Steel production uses large quantities of aluminum and calcium, some of which results in slag, a
5 waste byproduct composed mostly of alumina, lime, and trace metals (van Oss 2009). Slag is
6 then used as a raw material in the manufacturing of cement, another industry common to the
7 Flats. Other industries in this area include asphalt, gravel, petroleum, and aluminum processing,
8 along with road salt production and storage.

9 2.2 Site Selection

10 A method designed to optimize the capture of spatial variability in $PM_{10-2.5}$ was used to select
11 sampling sites. As described by Kumar, Chu et al. (2011), a preliminary 'demand surface' of PM_{10}
12 with a high spatial resolution (90 m) was generated for the study area, using the empirical
13 relationship between satellite-based aerosol optical depth and ground-based PM_{10}
14 measurements. PM_{10} was used as the best available surrogate for $PM_{10-2.5}$. Sites were identified
15 and ranked that would maximize the variability observed in the preliminary surface. This
16 approach, unlike classical sample site selection, was adopted to minimize redundancy in sites by
17 controlling for spatial autocorrelation. The locations of optimal sites were adjusted by moving
18 them to the closest schools, churches, fire stations, and private homes as practical for logistic
19 and security reasons. One sampler was damaged during the first week, and this site was
20 dropped from the remainder of the study, leaving a total of 25 sites for the study.

21 2.3 Sampling and Sample Analysis

22 A UNC passive aerosol sampler (Wagner and Leith 2001) housed in a protective shelter (Ott and
23 Peters 2008) was deployed for one week at each site over three consecutive weeks in August
24 2008. The shelter was designed to shield the passive sampler from precipitation and to minimize
25 dependence of particle deposition on wind speed. Samplers were changed out over a period of
26 three hours on Tuesday of each week. The weather over the study period was typical of summer
27 in this area and fairly consistent between weeks. Mean temperatures (Week 1: 22°C; Week 2:
28 23°C; and Week 3: 21°C) and mean relative humidity (Week 1: 64%; Week 2: 59%; and Week 3:
29 69%) were similar between weeks. Rainfall was observed only during Week 2 (3 mm during one
30 hour) and Week 3 (15 mm during one hour on two separate days). Winds from N and NNE were
31 observed on all weeks. The highest winds were from the SW in Week 1, from the NNE in Week
32 2, and from the E and SE in Week 3.

33 The size and elemental composition of individual particles deposited on the passive sampler
34 were determined by CCSEM-EDS. Samples were analyzed using a Personal SEM™ or PSEM (FEI
35 Aspex, Delmont, PA) (Hopke and Casuccio 1991). Each passive sample was coated with a thin
36 film (~ 200 Å) of conductive carbon to prevent sample charging during SEM analysis. The PSEM
37 was operated in the backscattered electron detection mode at an accelerating voltage of 20 kV.

1 Particles were detected rastering the electron beam across the sample surface until the
2 backscattered electron signal exceeded a preset background threshold level. Particles with
3 diameters between 1 μm and 15 μm were selected for further characterization including
4 measuring the particle size, acquiring a digital image of the particle, and collection of an EDS
5 spectrum to determine the particle's composition. The process of identifying and characterizing
6 particles was repeated until 1000 particles in the 1-15 μm size range were analyzed or until the
7 entire sample area was covered ($\sim 20 \text{ mm}^2$).

8 The mass of each particle was estimated by multiplying the particle volume by particle density.
9 Following Wagner and Leith (2001), a volume shape factor (1.6) was used to convert the
10 projected area diameter from SEM imaging to an equivalent volume diameter, which was then
11 used to compute particle volume. The density of the particle was estimated from analysis of x-
12 ray spectrum assuming that the particle was in the form of an oxide. An empirical deposition
13 velocity model was used to convert the deposited mass to ambient $\text{PM}_{10-2.5}$ (Wagner and Leith
14 2001, Ott, Cyrs et al. 2008). After CCSEM-EDS analysis, the particle micro-images were manually
15 reviewed as a quality check to reject false positive artifacts and to assist in particle classification
16 based on morphology (e.g., pollen).

17 2.4 Particle Classification

18 After analysis, particles were classified into groups with similar elemental composition using
19 rules based on the elemental composition of particles. Initially, pre-defined particle classification
20 rules were used and then modified to minimize the number of particles classified as
21 'Miscellaneous'. The final rules included 13 compositional classes as shown in Table 1. These
22 rules were applied sequentially top down, beginning with Rule 1, to sort particles into distinct
23 compositional classes: pollen, carbon-rich (C), sodium chloride (NaCl), sodium-rich (Na-rich),
24 calcium/sulfur rich (Ca/S-rich), silica/aluminum-rich (Si/Al-rich), iron-oxide (Fe oxide), aluminum-
25 rich (Al rich), silica-rich (Si-rich), metal rich (metal-rich), iron-rich (Fe-rich), calcium-rich (Ca-rich)
26 and a "catch all" (miscellaneous) class. Table 1 also provides a listing of potential sources of
27 particles in these classes in the Cleveland airshed. Images and EDS spectra of particles
28 representative of several compositional classes are shown in Supplemental Information (Figure
29 S1).

30 Following Leith et al. (2007), the limit of detection (LoD) by mass was calculated for $\text{PM}_{10-2.5}$ and
31 each of its components as the mean $\mu\text{g}/\text{m}^3$ concentration per blank (determined from three
32 field blanks and three trip blanks) plus three times the standard deviation. The limit of
33 quantitation (LoQ) by mass was determined as the mean concentration per blank plus ten times
34 the standard deviation. The percentage of sites having mean concentrations over the three
35 week sampling period greater than the LoD and LoQ were then determined. The results are
36 compiled by component in Table 2. The first column shows the mean number of particles with
37 physical diameters between 1.5 μm and 15 μm (plus standard deviation) detected in blanks,
38 which may be useful for planning future studies. Nine components including $\text{PM}_{10-2.5}$ were
39 detected above the LoD at the majority of sites, but only $\text{PM}_{10-2.5}$, Ca-rich and Ca/Si exceeded

1 their LoQs at more than half the sites. For Ca/S, Ca/Si, Na-rich and Pollen, it was not possible to
2 determine LoDs and LoQs because no particles in this size range were detected in the blanks. As
3 a best guess for these components, we used the LoD and LoQs for NaCl, which had a similar
4 mean particle count in the blanks.

5 2.5 Spatial and Temporal Analysis

6 The Pearson correlation coefficient (r) was computed as an indicator of temporal correlation
7 among measurements at different sites. The correlation coefficient was computed in a
8 spreadsheet (Excel, Microsoft, Redmond, WA) from 300 site pairs. The spatial heterogeneity of
9 observed concentrations was investigated through graphical and quantitative analyses.
10 Normalized mean mass concentration maps were prepared to visually investigate the spatial
11 heterogeneity of $PM_{10-2.5}$ and each of its components. For each component, the normalized
12 mean mass concentration was calculated for each site by dividing the mean observed at that
13 site by the mean observed for all samples (3 weeks x 25 sites = 75). These normalized mean
14 concentrations were krigged and then plotted with mapping software (ArcMap Version 9.3,
15 Redlands CA).

16 Spatial heterogeneity was also investigated for each component using two quantitative
17 indicators: coefficient of divergence (COD) and percent spatial heterogeneity (SH%). Following
18 Wongphatarakul, Friedlander et al. (1998), COD was computed from 300 site pairs as follows:

19

$$COD_{jk} = \sqrt{\frac{1}{p} \sum_{i=1}^p \left(\frac{x_{ij} - x_{ik}}{x_{ij} + x_{ik}} \right)^2}$$

20 where x_{ij} and x_{jk} represent the mass concentration for week i at sampling site j , k is the number
21 of sites, and p is the number of observations. Following Li and Reynolds (1995), SH% was used as
22 an alternative approach to quantify spatial heterogeneity. SH% was calculated as:

$$SH\% = \frac{p_{sill}}{p_{sill} + nug} \times 100\%$$

23 where p_{sill} is the partial sill and nug is the nugget. The partial sill and the nugget were
24 determined from the a semivariogram of the natural log of concentrations using the
25 geostatistical wizard within mapping software (ArcMap Version 9.3, Redlands CA). The nugget
26 represents the random or stochastic component of the variability, the partial sill represents the
27 spatial heterogeneous component, and total variance (referred to as the sill) can be expressed
28 as $(p_{sill} + nug)$. Thus, SH% represents the portion of the total variance attributed to spatial
29 heterogeneity and highlights the presence of spatial structure within a data set (Wagner and
30 Fortin 2005).

1 2.6 Concentrations in Flats Compared to Valley and
2 Non-Valley Suburban Sites

3 Three sites were selected to compare concentrations observed in the Flats to those observed at
4 suburban locations. Site 20 located within the Cuyahoga River Valley was selected to represent
5 the Flats District. Site 30 was selected as a suburban background site within the Cuyahoga River
6 Valley, and Site 34 was selected as a suburban non-valley background site. Kruskal-Wallis one-
7 way analysis of variance (ANOVA) was used to compare the concentration means between Sites
8 20, 30 and 34 for each compositional class. Median concentration 95% confidence intervals
9 were generated (Minitab, Version 17, State College, PA) to compare the Flats industrial sites to
10 suburban background sites. Kruskal-Wallis analysis was conducted because the assumption of
11 normality was met for some of the components but not others and log-transformation of the
12 data did little to improve normality.

13 **3. RESULTS**

14 Normalized concentration maps are presented in Figure 2 for: a) $PM_{10-2.5}$; b) Si/Al-rich
15 component of $PM_{10-2.5}$; c) Ca-rich component of $PM_{10-2.5}$; and d) Fe-oxide component of $PM_{10-2.5}$.
16 These normalized plots allow visualization of spatial heterogeneity with dark regions indicating
17 concentrations greater than the mean and light regions indicating those less than the mean.
18 Actual concentrations observed for $PM_{10-2.5}$ and its components are shown in Figure 3c. $PM_{10-2.5}$
19 exhibited substantial heterogeneity with elevated concentrations observed in the river valley,
20 stretching from Lake Erie south through the central industrial area (Figure 2a). The composite
21 mean $PM_{10-2.5}$ over all sites was $22 \mu\text{g m}^{-3}$ with a range from 13 to $48 \mu\text{g m}^{-3}$. The highest $PM_{10-2.5}$
22 means were observed in the Flats ($35 \mu\text{g m}^{-3}$ at Site 1; $43 \mu\text{g m}^{-3}$ at Site 35; and $48 \mu\text{g m}^{-3}$ at Site
23 20), whereas lower means were observed to the west and east of this area. The lowest $PM_{10-2.5}$
24 means were observed at the suburban background sites ($13 \mu\text{g m}^{-3}$ at Site 34; and $15 \mu\text{g m}^{-3}$ at
25 Site 30). A similar elongated shape of higher concentrations in the Flats area was observed for
26 Ca-rich (Figure 2c) and Fe-oxide components of $PM_{10-2.5}$ (Figure 2d). In contrast, the spatial
27 distribution of the Si/Al-rich (Figure 2b) class was less heterogeneous compared to the other
28 compositional classes, although the highest values were still observed at the south end of the
29 Flats.

30 A quantitative indicator of spatial heterogeneity, COD, is presented for $PM_{10-2.5}$ and components
31 in Figure 3a. A COD of zero indicates no difference between site concentrations (homogeneous),
32 whereas a COD greater than 0.2 is considered to indicate substantial spatial heterogeneity
33 (Wilson et al. 2005). COD values fell into two distinct groups (high and low), but all components
34 had median CODs > 0.2 . Median CODs for the highest group ranged from 0.64 to 0.76 as follows
35 (COD values in parenthesis): metal-rich (0.64); Fe-rich (0.64); Ca/S-rich (0.65); Fe-oxide (0.66);
36 and Al-rich (0.76). Median CODs for the lowest group ranged from 0.24 to 0.39 as follows: $PM_{10-2.5}$
37 (0.24); C-rich (0.26); Si/Al-rich (0.29); Si-rich (0.32); miscellaneous (0.35); and Ca-rich (0.39).

1 Temporal associations for concentrations observed between sites can potentially be inferred
2 from Pearson correlation coefficient (r) determined from site pairs (300) over the three week
3 study (Figure 3b). Values of r can range from negative one to positive one with greater positive
4 values indicating a stronger temporal association in the concentrations observed at different
5 sites. For every $PM_{10-2.5}$ component, concentrations measured at one or more site pairs were
6 highly correlated (near 1) and highly anti-correlated (near -1), producing the wide range of r
7 values plotted in Figure 3b. $PM_{10-2.5}$ had a median r -value of 0.09, and median correlations were
8 within +/- 0.4 for all remaining components, except Ca-rich (median r = 0.6) and Si/Al-rich
9 (median r = 0.5).

10 Percent spatial heterogeneity (SH%) for $PM_{10-2.5}$ and its components are presented in Figure 4.
11 SH% ranged from 0% for Si/Al-rich to 100% for Fe-rich. SH% was near 100% for many
12 components (misc., pollen, Na-rich, Ca-rich, metal-rich, and Fe-rich) and for $PM_{10-2.5}$. SH% was
13 34% for Si-rich, between 55% and 65% for NaCl, C-rich, and Al-rich, and 80-85% for Fe-oxide and
14 Ca/S-rich.

15 In Figure 5, median concentrations of $PM_{10-2.5}$ and components observed in the Flats are
16 compared to valley and non-valley suburban sites. $PM_{10-2.5}$, Ca-rich, Ca/S-rich, Fe-rich, metal-rich
17 and miscellaneous concentrations observed in the Flats were substantially and statistically
18 higher than those observed at either suburban site. There was no statistical difference in Fe-
19 oxide, Si/Al rich, Si-rich, Al-rich, and C-rich concentrations when compared to Site 30. Compared
20 to background Site 34, concentrations observed at Site 20 within the Flats were significantly
21 higher for all compositional classes except Fe-oxide, Al-rich, and C-rich. For all classes except
22 Si/Al-rich and Al-rich, the variability in concentrations was greater within the Flats (Site 20) than
23 at suburban background sites. For all classes except Ca rich and miscellaneous, the variability in
24 concentrations was also greater at Site 30 than at Site 34.

25 **4. DISCUSSION**

26 This work demonstrates that some components of coarse particles are considerably more
27 spatially heterogeneous than other components and $PM_{10-2.5}$ mass in general. The Si/Al-rich
28 component of $PM_{10-2.5}$ was more evenly distributed throughout the airshed (Figure 2b) than
29 other components, such as Ca-rich (Figure 2c) and Fe-oxide (Figure 2d), with substantially higher
30 concentrations in the Flats compared to outlying areas. These visual observations of
31 heterogeneity were consistent with quantitative indicators of spatial heterogeneity.
32 Heterogeneity indicators for the Si/Al-rich component (COD = 0.3; SH% = 0%) were substantially
33 lower than the Ca-rich (COD = 0.4; SH% = 100%) and Fe oxide components (COD = 0.65; SH% =
34 80%). All median CODs exceeded 0.2, a level suggested by EPA to indicate substantial
35 heterogeneity (EPA 2004). The median COD for $PM_{10-2.5}$ mass was 0.25 with greater CODs
36 observed for all 13 components of $PM_{10-2.5}$. Median CODs for components ranged from 0.26 for
37 C-rich to 0.82 for pollen. Percent spatial heterogeneity (SH%) ranged from 0% (low spatial
38 heterogeneity) for Si/Al-rich to 100% (high spatial heterogeneity) for Fe-rich.

1 The COD results for PM_{10-2.5} mass observed in this study can be compared to those observed in
2 other cities. The median COD of 0.25 for PM_{10-2.5} mass is similar to values observed in Los
3 Angeles, CA [COD range: 0.15 to 0.33 (Krudysz, Froines et al. 2008); COD median: 0.24 (Pakbin,
4 Hudda et al. 2010)], Iowa City, IA (COD range: 0.21 to 0.36) (Ott, Kumar et al. 2008), and
5 Birmingham, United Kingdom (COD mean: 0.2 ± 0.1) (Lianou, Chalbot et al. 2007), but lower
6 than values observed in Rochester, NY (COD_{min}: 0.365; COD_{max}: > 0.7) (Lagudu, Raja et al. 2011).
7 Compared to the COD observed in this study, CODs for PM_{10-2.5} were higher in Helsinki, Finland
8 (COD mean: 0.5 ± 0.1) and Athens, Greece (COD mean: 0.6 ± 0.1) and lower in Amsterdam, The
9 Netherlands (COD mean: 0.07 ± 0.01) (Lianou, Chalbot et al. 2007).

10 Pearson correlation coefficients (Figure 3b) suggest that concentrations were not strongly
11 temporally associated. With only 3 data points per site pair, however, any correlations must be
12 viewed with caution. For most components, median correlations were near zero, indicating little
13 temporal association across the region over the three, week-long sampling periods. However,
14 median correlations for Ca-rich and Si/Al-rich classes were positively skewed with median r
15 values greater than 0.5, indicating some positive temporal relationship. The higher median
16 correlation for the Si/Al-rich class is consistent with a PM_{10-2.5} component that is more regional in
17 nature.

18 The spatial heterogeneity observed for components in this study are generally consistent with
19 suspected sources of coarse particles in Cleveland. Substantially higher concentrations were
20 observed in the Flats for Fe-oxide (Figure 2d) and Ca-rich components (Figure 2c). COD and SH%
21 values were relatively high for Si-rich, Al-rich, Fe-oxide, Fe-rich, Ca-rich, Ca/S-rich, C-rich, and
22 metal-rich components. These spatial patterns and higher quantitative indicators of
23 heterogeneity are consistent with emissions from steel and cement industries common in the
24 Flats.

25 Significantly higher concentrations for Ca-rich, Ca/S-rich, Fe-rich, and metal-rich components
26 observed in the Flats (Site 20) when compared to either background site (Figure 5) are
27 consistent with local emissions of coarse particles that tend to settle near the source. The band
28 of high concentrations in the map for the Ca-rich component (Figure 2c) is restricted to the flats
29 area suggesting limited transport. In contrast, there is evidence that the Fe-oxide component is
30 transported from the Flats along the Cuyahoga River Valley. The band of high concentrations for
31 Fe-oxide stretches along the entire valley to Site 30 (Figure 2d). As shown in Table S1, winds
32 from N and NNE were observed on all weeks, which could account for this transport. Further
33 analysis of correlations among meteorological data from multiple stations in the Cleveland area
34 and observed concentrations of the components of coarse particles will be the subject of a
35 future manuscript.

36 Those components with low spatial heterogeneity suggest regional or ubiquitous sources.
37 Relatively low COD and SH% values were observed for Si-rich (median COD = 0.3; SH% = 35) and
38 Si/Al-rich (median COD = 0.3; SH% = 0). These components are associated with crustal earth
39 material expected as a source prevalent throughout the airshed. As seen in Figure 2b, Si/Al-rich

1 concentrations were more evenly distributed than other components consistent with a more
2 broadly distributed regional source. Although not statistically significant, higher median
3 concentrations and greater variability in the Si/Al-rich component were observed at the Flats
4 and at the valley background site (Site 30) compared to the other background site (Site 34;
5 Figure 5). Compared to suburban environments where vegetation acts as a natural sink for PM,
6 there are substantially more hard paved surfaces, traffic volume, and density of buildings within
7 the Flats, which may enhance coarse particulate re-suspension. Possibly Si/Al-rich particles are
8 re-suspended and transported along the valley.

9 Percent relative spatial heterogeneity may be a more meaningful quantitative indicator of
10 heterogeneity than COD. Although COD and SH% provided consistent information in most cases,
11 SH% values were sometimes more consistent with visual interpretation of concentrations maps.
12 A visual rank order of the maps in Figure 2 from least to most spatial heterogeneity of the maps
13 is consistent with rank order by SH% but not COD: Si/Al-rich, SH% = 0, COD = 0.3 (Figure 2b); Fe-
14 oxide, SH% = 80, COD = 0.65 (Figure 2d); PM_{10-2.5}, SH% = 100, COD = 0.25 (Figure 2a); and Ca-rich,
15 SH% = 100, COD = 0.4 (Figure 2b). This finding is attributed to the fact that SH% is computed
16 from elements of the semivariogram, which by definition depicts the spatial autocorrelation in
17 data. Thus, SH% relates directly to spatial patterns in the data, whereas COD is a statistical
18 construct providing an indicator of measurement differences without regard to distance
19 between sites.

20 However, in the limited comparison of PM_{10-2.5} and Ca-rich, SH% as applied in this work is not as
21 sensitive as visual observation of the maps. For both, the SH% was 100, although visually PM_{10-2.5}
22 appears less spatially heterogeneous than Ca-rich. In this case, CODs were consistent with the
23 maps with COD = 0.25 for PM_{10-2.5} lower than COD = 0.4 for Ca-rich. More work is needed to
24 investigate ways to apply information from the semivariogram to arrive at a more sensitive
25 estimate of spatial heterogeneity.

26 Our results are limited to a three-week period in one season and may not be representative of
27 coarse particle concentrations in this airshed more generally. Also, the samples collected in this
28 study were limited to a one week sampling duration, which for many samples resulted in
29 particle loadings that were low for CCSEM-EDS analysis. The analysis of LoD and LoQ
30 summarized in Table 2 provides important information for future work. These results reinforce
31 the importance of clean blanks and adequate sampling time. LoDs and LoQs would be lower had
32 the blank substrates used in this work been cleaner, and the average particle counts for each
33 component measured in the field samples would be greater for sampling times longer than one
34 week. Longer sampling times, two weeks or more, may have been more appropriate from a
35 particle loading perspective and aligned with the study of chronic health effects. Alternatively, a
36 passive sampler with a larger collection surface would provide more particles for analysis for the
37 study of short-term health effects.

38 In conclusion, a network of passive samplers analyzed by CCSEM-EDS was used to determine the
39 spatial variability of PM_{10-2.5} and its components in Cleveland, OH. The concentrations of some

1 PM_{10-2.5} components were substantially more spatially heterogeneous than others. PM_{10-2.5} and
2 components associated with steel and cement production (Fe-oxide and Ca-rich) were higher in
3 the industrial Flats district, whereas those components associated with crustal earth material
4 (Si/Al-rich) were more uniformly observed throughout the airshed. There is some evidence that
5 certain components are transported from the industrial Flats to downwind suburban valley
6 sites. Lastly, percent spatial heterogeneity (SH%) may be a more meaningful indicator of
7 heterogeneity than the commonly used coefficient of divergence (COD). SH% leverages the
8 underlying spatial autocorrelation in a dataset being calculated from components of the
9 semivariogram, whereas the COD is a statistical construct that does not account for the
10 distances between sites.

11 These findings demonstrate the potential of a passive sampling network coupled with
12 automated single particle analysis to assess the spatial and temporal variability of PM_{10-2.5} mass
13 and composition. This measurement methodology could substantially reduce exposure
14 misclassification in the epidemiological study of adverse health effects associated with exposure
15 to PM_{10-2.5}. The methodology may also be a valuable tool to attribute observed concentrations
16 to specific sources.

17 **ACKNOWLEDGMENTS**

18 The authors thank the numerous support staff of EPA Region 5, Cleveland Department of Air
19 Quality, and Alion Science and Technology that were involved in deployment and retrieval of
20 passive samplers. The United States Environmental Protection Agency through its Office of
21 Research and Development funded and collaborated in the research described here under
22 contracts EP09D000463 and EP11D000010 to the University of Iowa. It has been subjected to
23 Agency review and approved for publication.

24

1 **REFERENCES**

- 2 Adar, S. D., P. A. Filigrana, N. Clements and J. L. Peel (2014). "Ambient Coarse Particulate Matter
3 and Human Health: A Systematic Review and Meta-Analysis." Current environmental
4 health reports **1**(3): 258-274.
- 5 Ault, A. P., T. M. Peters, E. Sawvel, G. Casuccio, R. Willis, G. Norris and V. H. Grassian (2012).
6 "Single Particle SEM-EDX Analysis of Iron-Containing Coarse Particulate Matter in an
7 Urban Environment: Sources and Distribution of Iron within Cleveland, Ohio."
- 8 Brook, R. D., S. Rajagopalan, C. A. Pope, J. R. Brook, A. Bhatnagar, A. V. Diez-Roux, F. Holguin, Y.
9 Hong, R. V. Luepker and M. A. Mittleman (2010). "Particulate matter air pollution and
10 cardiovascular disease an update to the scientific statement from the American Heart
11 Association." Circulation **121**(21): 2331-2378.
- 12 Burton, R., H. Suh and P. Koutrakis (1996). "Spatial variation in particulate concentrations within
13 metropolitan Philadelphia." Environ. Sci. Technol **30**(2): 400-407.
- 14 Chang, H. H., R. D. Peng and F. Dominici (2011). "Estimating the acute health effects of coarse
15 particulate matter accounting for exposure measurement error." Biostatistics: kxr002.
- 16 Cheung, K., N. Daher, W. Kam, M. M. Shafer, Z. Ning, J. J. Schauer and C. Sioutas (2011). "Spatial
17 and temporal variation of chemical composition and mass closure of ambient coarse
18 particulate matter (PM_{10-2.5}) in the Los Angeles area." Atmospheric
19 Environment **45**(16): 2651-2662.
- 20 Cheung, K., M. R. Olson, B. Shelton, J. J. Schauer and C. Sioutas (2012). "Seasonal and spatial
21 variations of individual organic compounds of coarse particulate matter in the Los Angeles
22 Basin." Atmospheric Environment **59**: 1-10.
- 23 Fruin, S., R. Urman, F. Lurmann, R. McConnell, J. Gauderman, E. Rappaport, M. Franklin, F. D.
24 Gilliland, M. Shafer and P. Gorski (2014). "Spatial variation in particulate matter
25 components over a large urban area." Atmospheric Environment **83**: 211-219.
- 26 Goldman, G. T., J. A. Mulholland, A. G. Russell, M. J. Strickland, M. Klein, L. A. Waller and P. E.
27 Tolbert (2011). "Impact of exposure measurement error in air pollution epidemiology:
28 effect of error type in time-series studies." Environ Health **10**: 61.
- 29 Hoek, G., R. M. Krishnan, R. Beelen, A. Peters, B. Ostro, B. Brunekreef and J. D. Kaufman (2013).
30 "Long-term air pollution exposure and cardio-respiratory mortality: a review." Environ
31 Health **12**(1): 43.
- 32 Hopke, P. K. and G. Casuccio (1991). Scanning electron microscopy. Receptor modeling for air
33 quality management, Elsevier. **7**.

- 1 Kelly, F. J. and J. C. Fussell (2012). "Size, source and chemical composition as determinants of
2 toxicity attributable to ambient particulate matter." Atmospheric Environment **60**: 504-
3 526.
- 4 Krudysz, M., J. Froines, P. Fine and C. Sioutas (2008). "Intra-community spatial variation of size-
5 fractionated PM mass, OC, EC, and trace elements in the Long Beach, CA area."
6 Atmospheric Environment **42**(21): 5374-5389.
- 7 Kumar, N., A. D. Chu, A. D. Foster, T. Peters and R. Willis (2011). "Satellite remote sensing for
8 developing time and space resolved estimates of ambient particulate in Cleveland, OH."
9 Aerosol Science and Technology **45**(9): 1090-1108.
- 10 Lagudu, U. R. K., S. Raja, P. K. Hopke, D. C. Chalupa, M. J. Utell, G. Casuccio, T. L. Lersch and R. R.
11 West (2011). "Heterogeneity of coarse particles in an urban area." Environmental science
12 & technology **45**(8): 3288-3296.
- 13 Leith, D., D. Sommerlatt and M. G. Boundy (2007). "Passive sampler for PM10-2.5 aerosol."
14 Journal of the Air and Waste Management Association **57**(3): 332-336.
- 15 Li, H. and J. Reynolds (1995). "On definition and quantification of heterogeneity." Oikos: 280-
16 284.
- 17 Lianou, M., M.-C. Chalbot, A. Kotronarou, I. G. Kavouras, A. Karakatsani, K. Katsouyanni, A.
18 Puustinen, K. Hameri, M. Vallius and J. Pekkanen (2007). "Dependence of home outdoor
19 particulate mass and number concentrations on residential and traffic features in urban
20 areas." Journal of the Air & Waste Management Association **57**(12): 1507-1517.
- 21 Ott, D., W. Cyr and T. Peters (2008). "Passive measurement of coarse particulate matter, PM10-
22 2.5." Journal of Aerosol Science **39**(2): 156-167.
- 23 Ott, D., N. Kumar and T. Peters (2008). "Passive sampling to capture spatial variability in PM10-
24 2.5." Atmospheric Environment **42**(4): 746-756.
- 25 Ott, D. and T. Peters (2008). "A Shelter to Protect a Passive Sampler for Coarse Particulate
26 Matter, PM 10-2.5." Aerosol Science and Technology **42**(4): 299-309.
- 27 Pakbin, P., N. Hudda, K. Cheung, K. Moore and C. Sioutas (2010). "Spatial and Temporal
28 Variability of Coarse (PM 10-2.5) Particulate Matter Concentrations in the Los Angeles
29 Area." Aerosol Science and Technology **44**(7): 514-525.
- 30 Seinfeld, J. H. and S. N. Pandis (2012). Atmospheric chemistry and physics: from air pollution to
31 climate change, John Wiley & Sons.
- 32 Thornburg, J., C. E. Rodes, P. A. Lawless and R. Williams (2009). "Spatial and temporal variability
33 of outdoor coarse particulate matter mass concentrations measured with a new coarse

- 1 particle sampler during the Detroit Exposure and Aerosol Research Study." Atmospheric
2 Environment **43**(28): 4251-4258.
- 3 van Oss, H. (2009). "Minerals Yearbook: Slag, Iron and Steel [Advance Release]." US Geological
4 Survey.
- 5 Wagner, H. H. and M.-J. Fortin (2005). "Spatial analysis of landscapes: concepts and statistics."
6 Ecology **86**(8): 1975-1987.
- 7 Wagner, J. and D. Leith (2001). "Passive aerosol sampler. Part I: Principle of operation." Aerosol
8 Science and Technology **34**(2): 186-192.
- 9 Wongphatarakul, V., S. K. Friedlander and J. P. Pinto (1998). "A comparative study of PM2.5
10 ambient aerosol chemical databases." Environmental Science and Technology **32**(24):
11 3926-3934.
- 12 Zhang, L. and Z. He (2014). "Technical Note: An empirical algorithm estimating dry deposition
13 velocity of fine, coarse and giant particles." Atmospheric Chemistry and Physics **14**(7):
14 3729-3737.
- 15

1 Table 1: Rules for sorting particles by composition into components of PM_{10-2.5}. Numbers
 2 shown in rules are the percentage of the given element with reference to the
 3 total x-ray spectrum.

Class #	Component	Rule	Potential Sources in the Cleveland Airshed
1	pollen	$P \geq 3$ and $Ca \geq 3$ and $C \geq 80$	Naturally occurring plant material
2	C-rich	$C \geq 50$	Material rich in carbon including plant material other than pollen, soot, tire rubber, etc.
3	NaCl	$(Na+Cl) > 70$ and $Na > 20$ and $Cl > 30$	Rivers and Lake Erie; Road salt (but unlikely in summer)
4	Na-rich	$Na \geq 40$	Salts; Lake Erie; Na-S from various industrial processes
5	Ca/S-rich	$Ca \geq 20$ and $S \geq 20$	Steel making; cement production; gypsum used in construction; by-product of atmospheric reaction of Ca with S.
6	Si/Al-rich	$Si \geq 30$ and $Al \geq 10$	Crustal material consistent with soil, road dust, fly ash
7	Fe-oxide	$Fe \geq 75$	Spherical: combustion processes used in steel making; coal fired power plants; Non-spherical: steel making; rust
8	Al-rich	$Al \geq 70$	Aluminum manufacturing; contamination from the sampler or shelter
9	Si-rich	$Si \geq 60$	Crustal material consistent with soil (quartz)
10	metal-rich	$Ti > 5$ or $Cr > 5$ or $Mn > 5$ or $Ni > 5$ or $Cu > 5$ or $Zn > 5$ or $Ba > 5$ or $Pb > 5$	Various industrial sources including steel making or coal-fired power plants; Cu, Ba, Zn may be from brake and tire wear; Ti, Mn and Ba may also be related to crustal material
11	Fe-rich	$Fe \geq 40$	Steel making (potential kish); rust
12	Ca-rich	$Ca \geq 40$	Naturally occurring crustal material (calcium carbonate or calcium oxide); steel making; cement production; construction activities
13	miscellaneous	Catch all	

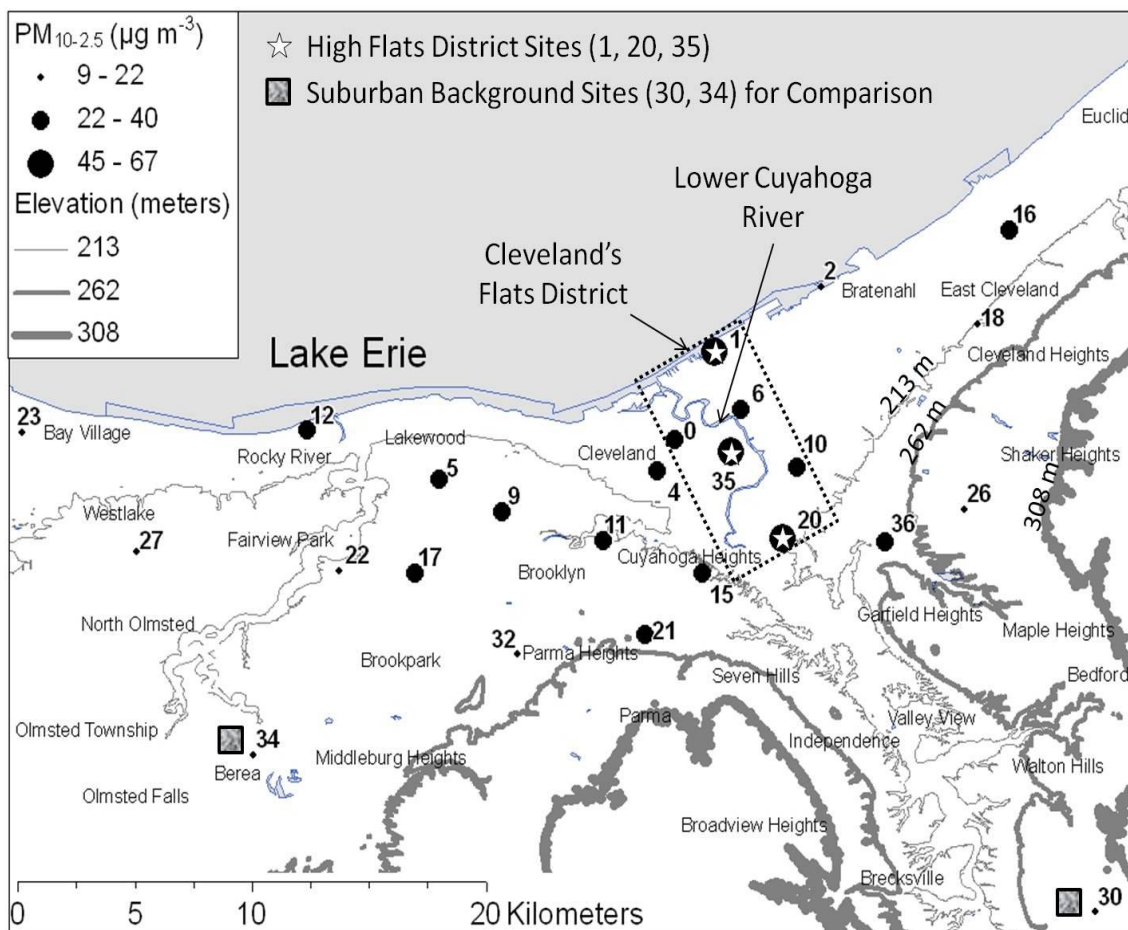
4

5

1 Table 2: Summary of blank analysis conducted to determine limit of detection (LoD) and
 2 limit of quantitation (LoQ). Components marked with * were absent in the blanks in the
 3 2.5–10 μm size range. The LoD and LoQ values for these components were estimated to
 4 be similar to those for NaCl, which had a similar number of mean blank counts in the 1.5-
 5 15 μm size range.
 6

Component	Blank Counts Mean (Std. Dev)	LOD ($\mu\text{g}/\text{m}^3$)	LOQ ($\mu\text{g}/\text{m}^3$)	%sites > LoD	%sites > LoQ
PM10-2.5	60 (37)	1.4	3.4	100	100
Ca-rich	1.2 (1.0)	0.12	0.37	100	100
Ca/Si*	0 (0)	~ 0.14	~0.40	100	60
Ssteel	0.3 (0.5)	0.01	0.03	76	48
Al-Si	1.3 (1.0)	0.43	1.28	96	44
Fe-rich	1.3 (1.2)	0.05	0.14	96	44
Fe-oxide	1.5 (0.5)	0.08	0.22	92	40
Si-rich	8.8 (7.5)	0.70	1.89	100	32
Misc.	1.5 (1.5)	0.07	0.20	84	32
Ca/S*	0.2 (0.4)	~ 0.14	~0.40	40	4
Al-rich	1.7 (2.3)	0.16	0.50	36	0
Metal-rich	5.7 (6.2)	0.58	1.59	32	0
C-rich	35.7 (30.4)	0.38	1.05	20	0
Na/Cl	0.3 (0.5)	0.14	0.40	4	0
Na-rich*	0.2 (0.4)	~ 0.14	~0.40	0	0
Pollen*	0.5 (0.5)	~ 0.14	~0.40	0	0

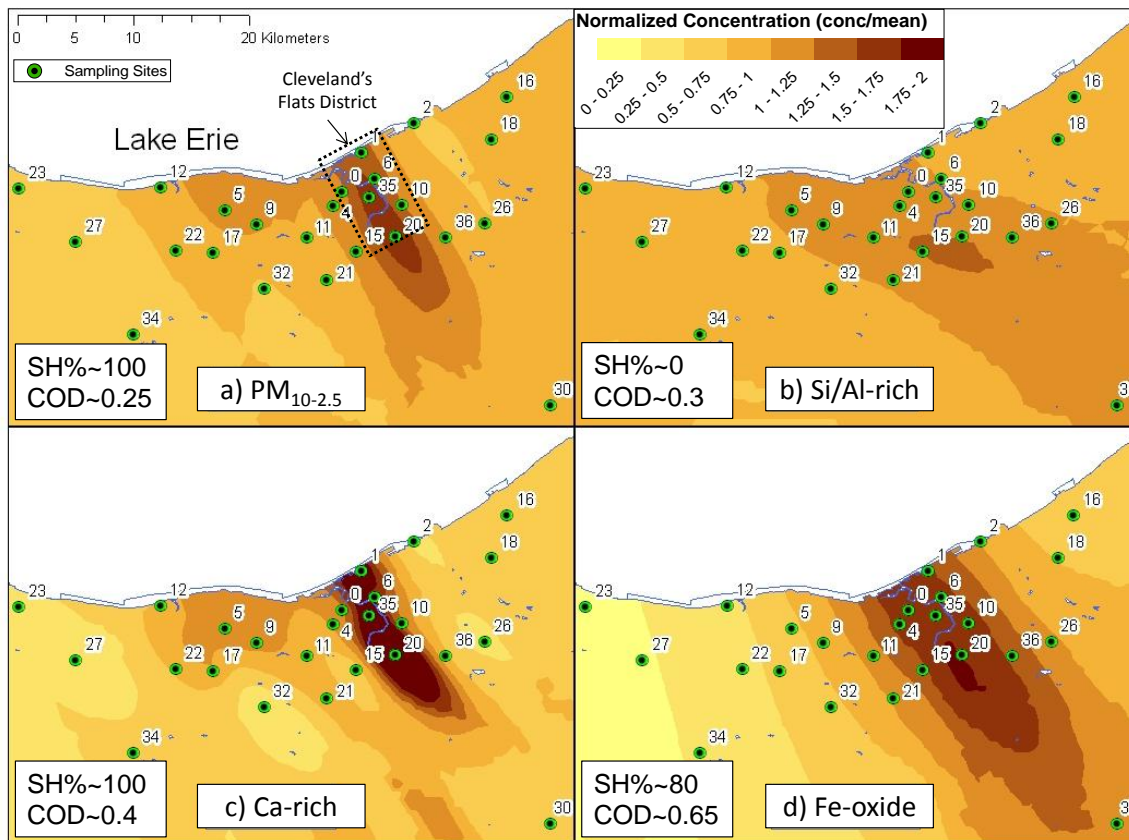
7



1

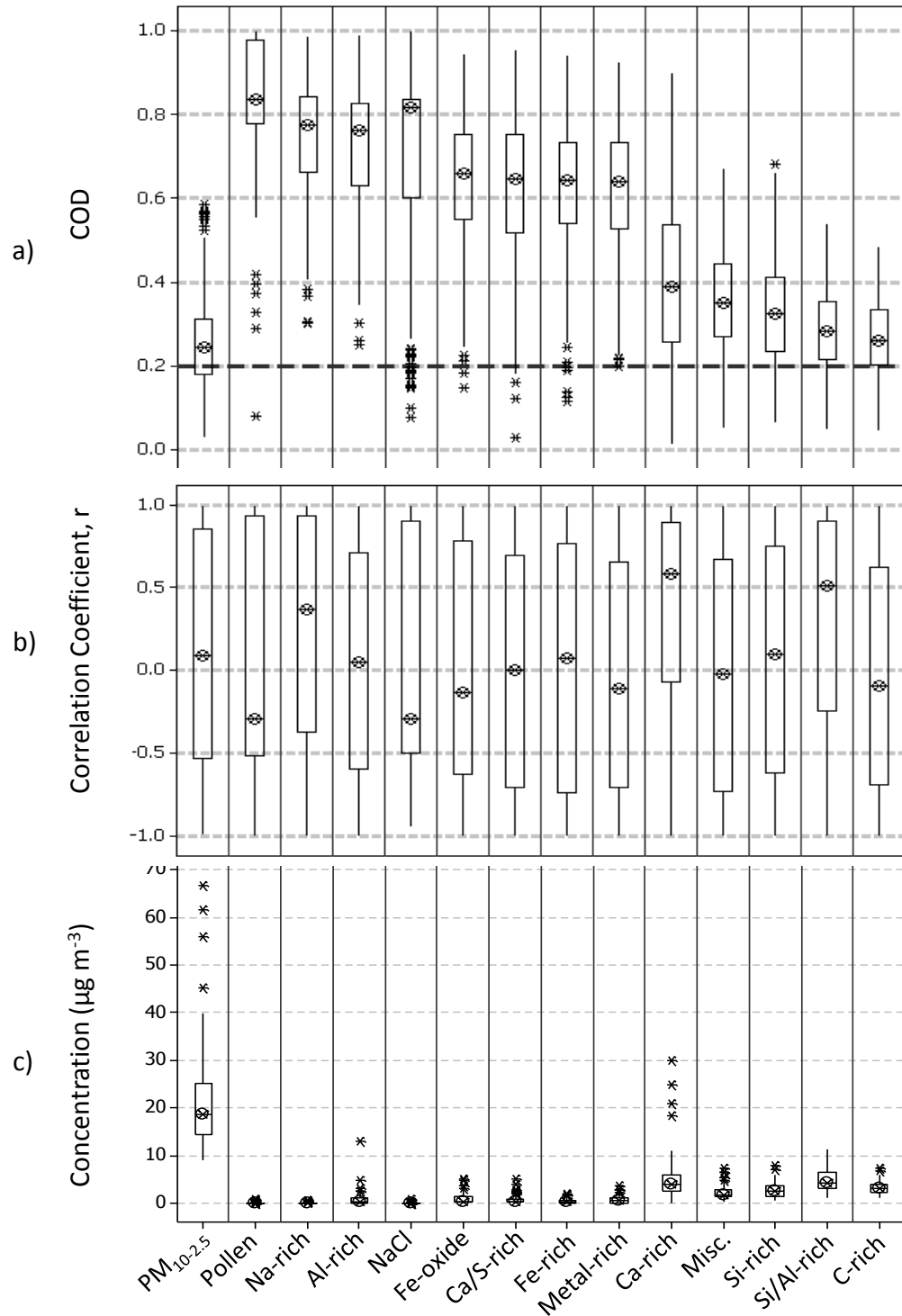
2 Figure 1: Map of Cuyahoga County, OH showing passive sampler locations and PM_{10-2.5}
 3 concentrations by site. Key reference points are identified: Lake Erie,
 4 Cleveland's Flats District (dotted line rectangle), Lower Cuyahoga River, high
 5 PM_{10-2.5} in the Flats (Sites 1, 20, 35), and comparison suburban sites (valley
 6 Site 30; non-valley Site 34). Elevation contours are lines weighted by
 7 thickness: 213 m (line thickness light), 262 m (line thickness medium), and
 8 308 m (line thickness heavy). Numbers represent sample site identification
 9 number and names represent municipal boundaries.

10



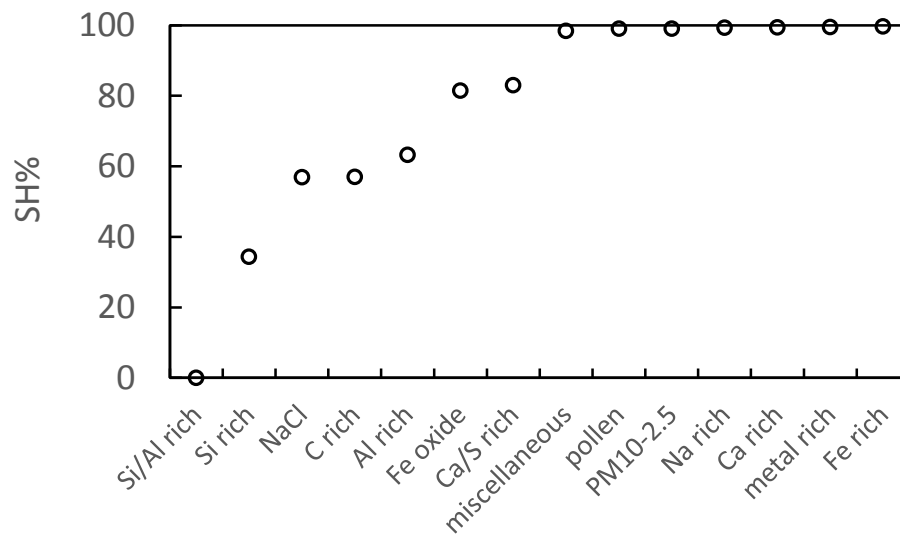
1

2 Figure 2: Maps of normalized concentration for: (a) $PM_{10-2.5}$; (b) Si/Al-rich; (c) Ca-rich;
 3 and (d) Fe-oxide. Normalized concentration scale bar in panel b applies to all
 4 maps. Dots with numbers represent sample locations and identification
 5 number.
 6



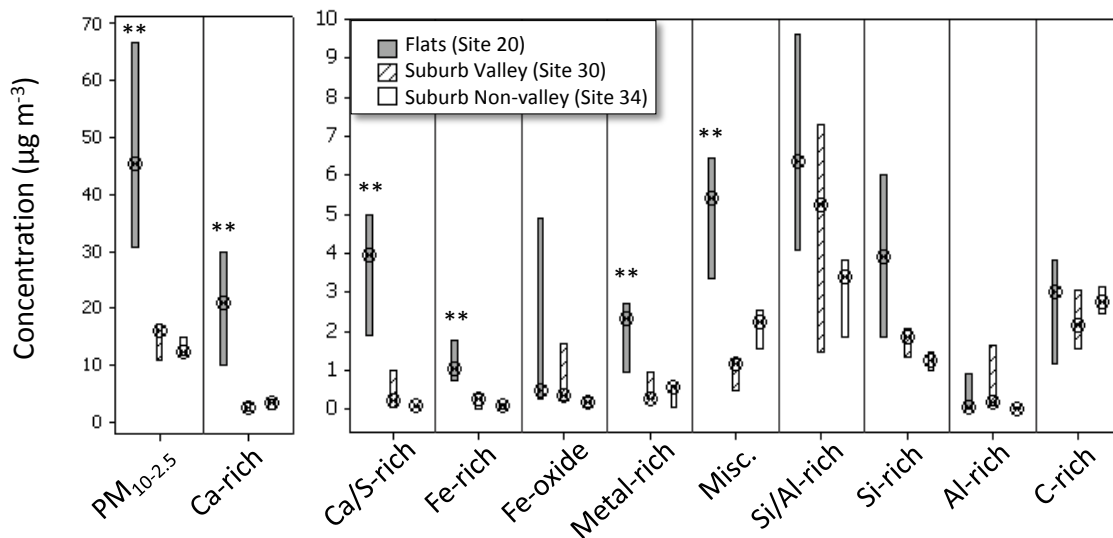
1 Figure 3: Coefficient of divergence (COD) by compositional class (a: top plot). COD
 2 values greater than 0.2 (bold dashed line) are considered spatially
 3 heterogeneous. Pearson correlation (*r*) by compositional class (b: middle plot).
 4 Concentration ($\mu\text{g m}^{-3}$) by compositional class (c: bottom plot). Box plots
 5 represent minimum, maximum, 1st and 3rd quartiles, outliers, and medians.

1
2



3
4
5
6

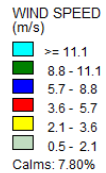
Figure 4: Percent spatial heterogeneity composite for all weeks for PM_{10-2.5} and by component.



1 Figure 5: Concentrations of PM_{10-2.5} and components observed at the Flats District (Site
 2 20) compared to those observed at Valley Suburban (Site 30) and Non-Valley
 3 Suburban (Site 34) sites. Box plots represent medians and 95% confidence
 4 intervals for the medians. Double asterisk (**) indicate that the medians were
 5 significantly different with a p-value < 0.08.

1 **Table S1.** Summary of meteorological data from Cleveland Hopkins International Airport.

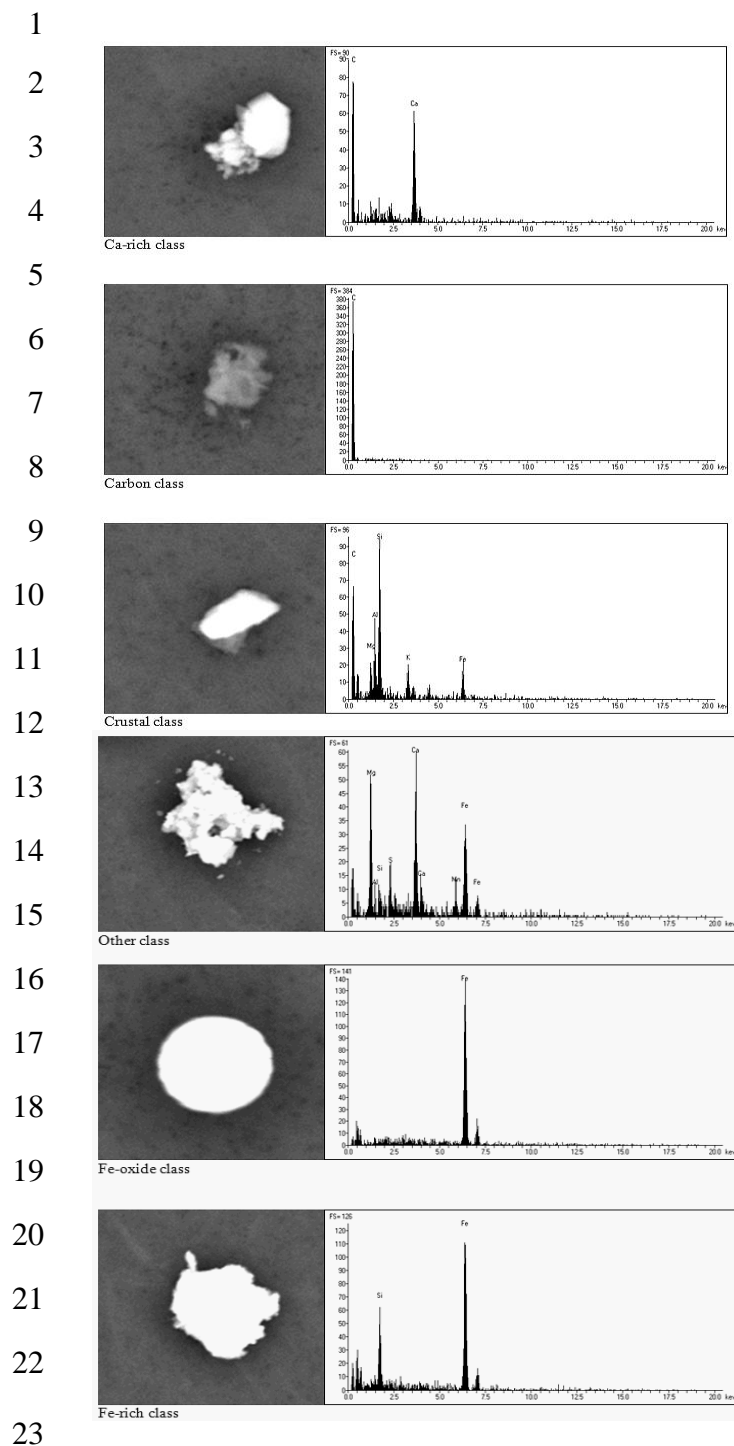
	Week 1 8/12/2008 – 8/19/2008			Week 2 8/19/2008 – 8/26/2008			Week 3 8/26/2008 – 9/2/2008		
Wind^a									
Rainfall Total, mm	0			3			15		
	Min	Mean	Max	Min	Mean	Max	Min	Mean	Max
Temp, C	13.0	21.5	29.0	13.0	22.7	32.3	13.9	21.1	29.4
RH, %	31	64	93	24	59	90	27	69	96



2 ^a direction from which the wind was blowing

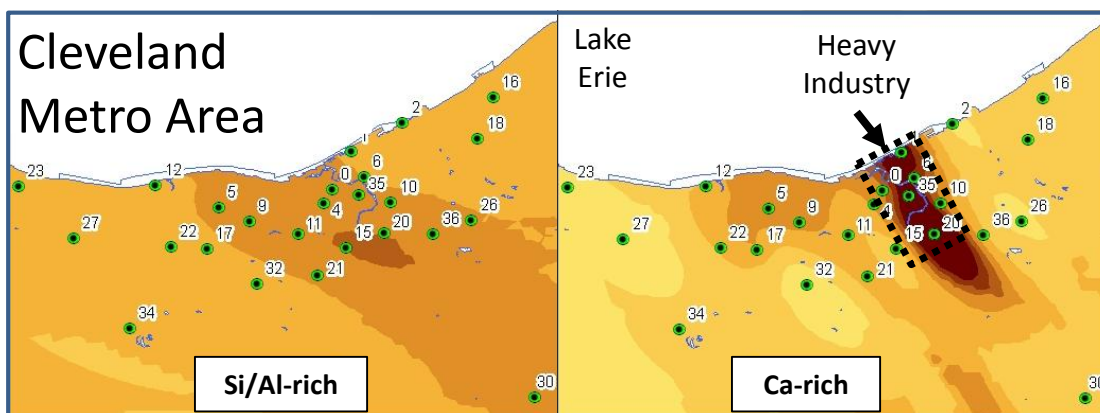
3

4 Data were obtained from <http://www.epa.ohio.gov/dapc/model/modeling/metfiles.aspx> as AERMOD surface files (SFC). Wind roses were
 5 prepared using WRPlot (Version 7.0, Lakes Environmental). Descriptive statistics on rainfall and temperature were compiled using MiniTab
 6 (Version 17.1).



24 **Figure S1:** X-ray spectra and scanning electron microscopy images of individual
25 particles. These include: Ca rich, carbon, crustal, miscellaneous (other), Fe
26 oxide, and Fe rich classes.

1 Graphical Abstract
2



3

HIGHLIGHTS

- Examined spatial variability of PM_{10-2.5} and components in Cleveland, OH.
- Used passive samplers with automated microscopy to classify particles.
- Components associated with steel and cement production highest in industrial area.
- Components associated with crustal material more uniformly distributed.
- Method may be useful to reduce exposure misclassification in epidemiological studies.